# TagSheet: Sleeping Posture Recognition with an Unobtrusive Passive Tag Matrix

Jia Liu[†] Xingyu Chen[†] Shigang Chen[‡] Xiulong Liu[§] Yanyan Wang[†] Lijun Chen[†]
[†]State Key Laboratory for Novel Software Technology, Nanjing University, China
[‡]Department of Computer & Information Science & Engineering, University of Florida, USA
[§]Department of Computing, The Hong Kong Polytechnic University, China
Email: jialiu@nju.edu.cn, sgchen@cise.ufl.edu, xiulongliudut@gmail.com, chenlj@nju.edu.cn

***Abstract*—Sleep monitoring plays an important role in many medical applications, including SIDS prevention, care of patients with pressure ulcers, and assistance to patients with sleep apnea, where studies have shown that autonomous and continuous monitoring of sleep postures provides useful information for lowering health risk. Existing systems are designed based on electrocardiogram, cameras and pressure sensors, which are expensive to deploy, intrusive to privacy, or uncomfortable to use. This paper presents TagSheet, the first sleep monitoring system based on passive RFID tags, which provides a convenient, non-intrusive, and comfortable way of monitoring the sleeping postures. It does not require attaching any tag directly to a patient's body. Tags are taped under a bed sheet. With a combination of hierarchical recognition, image processing and polynomial fitting, the proposed system identifies body postures based on the observed variation caused by the patient body to the backscattered signals from tags. The system does not require any personalized data training, making it plug-n-play in use. One additional advantage is that the system can also estimate the patient's respiration rate. This is particularly helpful in assisting patients with sleep apnea. We have implemented a prototype system, and experiments show that the system performs posture identification with an accuracy up to 96.7% and in the meantime it measures the respiration rate with a small error of about 0.7 bpm (breath per minute).**

## I. Introduction

We spend one third of our lives in sleeping, which plays a vital role in good health and well-being. Clinical evidence suggests that body posture during sleep serves as a diagnostic indicator for a variety of chronic diseases and as an aid in medical therapies. One example is the sudden infant death syndrome (SIDS) for unexplained deaths of small children less than one year of age. As 1,545 US infants died from SIDS in 2014, studies showed that this risk would be much lower if infants were sleeping on their backs [1]. Pressure ulcers, also known as pressure sores, are a common clinical issue for bedridden patients in hospitals and care institutions [2]. These are skin injuries caused by prolonged stay in the same sleeping posture. To reduce the risk of developing pressure ulcers, caregivers must adjust the patients' postures every two hours to relieve their skin pressure. As patients may unconsciously move their positions from time to time, a system that continuously monitors the durations in different postures will provide caregivers with information on the best postures that they should adjust the patients to. In yet another example, sleep apnea is a sleep disorder characterized by pauses in breathing or periods of shallow breathing during sleep [3]. Prior studies have discovered the relationship between body postures and sleep apnea, and observed that avoidance of supine posture (i.e., sleeping on back) results in a decrease in the number and the severity of obstructive sleep apnea [4], [5]. A system that monitors both sleeping posture and breathing will help assess a patient's sleeping habit and the effectiveness of a certain sleeping aid/therapy.

In the above examples, autonomous and continuous monitoring of body postures during sleep provides useful information for lowering health risk due to inappropriate sleeping postures. To date, existing research has proposed a variety of approaches to monitor sleeping postures. Lee et al. [6] perform posture recognition based on cardiovascular signals from electrocardiogram. This approach requires specialized medical instrument and trained professionals, which make it expensive. Video cameras have also been used to recognize sleeping postures [7]. This image-based approach works but suffers from three drawbacks. First, the use of camera raises privacy concern, especially in a private environment, e.g., bedroom. While patients are likely to be comfortable to share electrocardiograms and other sensor data, video of private life is a different story. Second, it is hard for the camera to capture the posture image when the body is covered by the quilt. Third, people usually sleep at night. Darkness degrades video quality. Even when infrared cameras are used, video may still suffer from non-uniformity and artifacts. More recently, research has shifted to pressure sensing techniques [4], [8]. By designing a pressure sensitive bedsheet with densely deployed textile sensors, they are able to capture the pressure mapping images and recognize different postures using classifiers. However, these approaches require users to replace their mattresses with the pressure sensor mats or fix the sensor sheets to the surface of the mattresses, which could affect the patents'


Fig. 1. Chronic diseases related to sleeping postures.

sleeping comfort. Pressure sensors need a power supply such as batteries, which not only increases deployment cost, but also makes it difficult to miniaturize the sensors to a level that the users will not feel when laying on top of them.

In this paper, we present an RFID-based (radio frequency identification) system called *TagSheet* that provides a non-intrusive way of recognizing body postures without affecting users' sleeping comfort. TagSheet consists of passive tags that are taped under a bed sheet or on the surface of a mattresses, arranging in rows and columns to form a rectangular tag matrix, as shown in Fig. 2. Passive tags are powered by RF waves from an RFID reader, and they communicate with the reader by backscattering the RF signals. They are thin, flexible, and unnoticeable to users when separated with a sheet. The presence of a body between some tags and the reader will alter the backscattered RF signals from those tags to the reader, depending on the relative tag-body placement. By observing the RF signal variance amongst all tags, the reader is able to construct a coarse-grained grayscale snapshot, from which the sleep posture will be deduced. As the reader continuously interrogates the tags, it forms snapshot after snapshot over time, allowing continuous monitoring. Compared to the prior work, TagSheet has many advantages: It is battery-free, non-intrusive to privacy, and comfortable to use as we do not attach tags to human body; they are under a bed sheet. These advantages do not come for free. Due to its low resolution, analyzing an RF snapshot taken by TagSheet is much more challenging than doing so for a visual image or a dense pressure mapping. Adding to the challenge, we want to improve the usability of TagSheet by avoiding tedious personalized data training that is often needed by the traditional classification methods.

To meet the above challenge, we propose a hierarchical recognition scheme that gradually identifies sleeping postures from a coarse-grained subsumption to each individual posture output, without any training process needed, making TagSheet plug-and-play. We begin with generic posture analysis and define their geometric features present in RF snapshots. These features are derived as inherit physical characteristics of certain postures and thus they are universally applicable to different persons. By combining image processing and polynomial fitting, TagSheet achieves high accuracy in posture recognition. Moreover, as a by-product, TagSheet can also estimate the respiration rate, without requiring any extra hardware. This is useful as an additional indicator for assessing the physical health of a patient under posture monitoring. Our system is different from TagBreathe [9] in that we do not attach any tag to a user's chest as TagBreathe does. Finally, we examine the practical issues of how to choose proper tags that will produce the needed signal variation, how to avoid signal interference caused by occasional limb movement, and how to address the under-sampling problem by using selective reading. Summarized below, our contributions are three-fold.

1) We design a novel sleep monitoring system called TagSheet that provides a convenient, non-intrusive, and comfortable way of identifying the sleeping postures with a battery-free passive tag matrix, in complement to existing approaches based on electrocardiogram, cameras and pressure sensors, which have their limitations in practical use.


Fig. 2. System deployment of TagSheet.

2) We propose a hierarchical recognition scheme that gradually identifies the sleeping postures from a coarse-grained subsumption to each individual posture output, without any personalized training process needed, thus allowing plug-n-play deployment for different individuals. Besides, we incorporate a tag selection approach and a wavelet-filter based technology to produce a by-product function for estimating a user's respiration rate.

3) We implement a prototype of TagSheet. Extensive experiments show that the system performs posture identification with an accuracy up to 96.7% and in the meantime it measures the respiration rate with a small error of about 0.7 bpm (breath per minute). These promising results demonstrate the practical potential of using TagSheet as an unobtrusive tool for monitoring sleeping postures as well as breathing rate.

## II. TagSheet

### A. System Deployment

We design TagSheet as a set of passive tags taped on a thin and flexible carrier (e.g., bed sheet or plastic film under the sheet), making it easy to deploy on the mattress and unobtrusive to sleepers. Tags attached to the carrier are positioned in rows and columns, forming an $M$-by-$N$ rectangular matrix $A = \{a_{m,n}\}$, where $a_{m,n}$ denotes the tag at the $m$-th row and the $n$-th column of the matrix, $1 \leq m \leq M$, $1 \leq n \leq N$. The total number of tags is $M \times N$. Since the unit price of a passive tag is only a few cents, the total cost of TagSheet is low. For example, a TagSheet with 500 tags costs about 30 dollars. Above the TagSheet (bed), an RFID reader (antenna) hangs from the ceiling and collects tag IDs and RSSI (Received Signal Strength Indicator) measurements from those tags continuously, as shown in Fig. 2. During the use of TagSheet, the time is evenly split into a sequence of windows $T = \{t_1, t_2, t_3, ...\}$. At each time window $t_i$, $i > 0$, the reader constructs an RSSI snapshot $R_i = \{r^i_{m,n}\}$ based on tags' responses, where $r^i_{m,n}$ is the mean of RSSI measurements of tag $a_{m,n}$ within the window $t_i$. Besides, we let $R_0$ be the initial snapshot (which is also called *empty snapshot*) that consists of the RSSI values of all tags when nobody lies in bed.

Our problem in this paper is to recognize six sleeping postures, i.e., *supine, prone, left log, right log, left foetus, and right foetus*, from each snapshot $R_i$, $i \geq 0$. According to Idzikowski's study [10], these six postures are the most common postures. As shown in Fig. 3, the supine posture means lying horizontally with the face and torso facing up

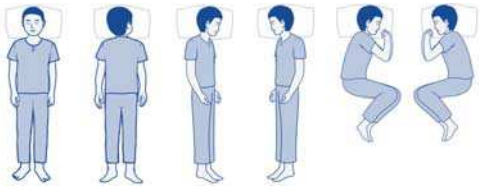

(a) (b) (c) (d) (e) (f)

Fig. 3. Six common sleeping postures [10]: (a) supine, (b) prone, (c) left log, (d) right log, (e) left foetus, (f) right foetus.

(8%), as opposed to the prone position, which is facing down (7%). A log means sleeping on left side (left log) or right side (right log) with arms and legs straight, which is the second most popular position (28%). The foetus is lying side with knees bent and arms stretched outwards, which is the most common sleeping posture (41%). If facing left, it is left foetus; otherwise, right foetus. We stress that although there are many kinds of variations of sleeping postures, these six postures cover the most cases in our daily lives and are sufficient to provide us with useful diagnostic information.

### B. Snapshot Difference

In TagSheet, since the relative location of the reader antenna and tags is fixed, the RF signals backscattered from each tag nearly remain stable in a static environment. When a person lies in bed (above the tag matrix), the human body that is made up primarily of "salt water" acts as an absorber of RF energy. That means the signals emitted by tags below the human body are very likely to be blocked by the human body, which makes the reader fail to collect the tag IDs and the corresponding RSSI values. Consider any tag $a_{m,n}$ at a time window $t_i$. If the tag is exactly under the body and is completely blocked, no response of $a_{m,n}$ will be received by the reader. In this case, we set RSSI value $r^i_{m,n}$ in the time window $t_i$ to a threshold $R^T$, which is less than the maximum receive sensitivity determined by the reader. For example, the maximum receiver sensitivity of Impinj Speedway R420 [11] is $-84$ dBm, so the threshold $R^T$ is less than $-84$ dBm when Impinj Speedway R420 is put into use for TagSheet.

Another impact of human body is reflection influence. The human body can be treated as a passive virtual transmitter that emits the reflected signals. These reflected signals and the line-of-sight signals from the reader will be superposed at the position of each tag, leading to destructive interference or constructive interference. Therefore, in consideration of the dual impacts of the human body, we attempt to use RSSI variances to recognize the sleeping posture. Specifically, the difference $\hat{R}_i$ between RSSI snapshot $R_i$ and the empty snapshot $R_0$ is served as the clue to figure out the body posture in the time window $t_i$.

$$\hat{R}_i = |R_i - R_0| = \{|r^i_{m,n} - r^0_{m,n}|\}, \tag{1}$$

where $1 \le m \le M$ and $1 \le n \le N$. The reason for not using $R_i$ directly is due to tag diversity and location diversity. Tag diversity is the hardware difference introduced during manufacturing, and location diversity is caused by varied distances and multipath effects to tags at different locations.

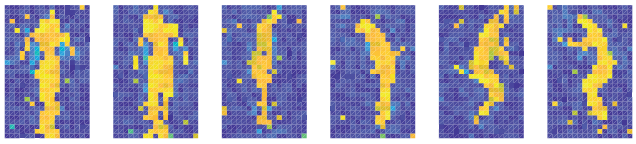

(a) (b) (c) (d) (e) (f)

Fig. 4. Snapshots of six sleeping postures: (a) supine, (b) prone, (c) left log, (d) right log, (e) left foetus, (f) right foetus.

We performed an experiment, which shows that the RSSI values of 20 different tags located at the same position vary from $-49$ dBm to $-45$ dBm, and that the RSSI values of the same tag at 20 different positions in a $5 \times 4$ matrix vary from $-59$ dBm to $-36$ dBm. Combining these two effects, when 20 different tags are placed at 20 different locations, their RSSI values vary from $-61$ dBm to $-34$ dBm. These results confirm that tag diversity and location diversity have great impact on RSSI measurement. We mitigate such impact by subtracting the empty snapshot $R_0$ from $R_i$, which removes tag/location diversity captured in $R_0$, while leaving the signal fingerprint left by the presence of human body.

Fig. 4 shows the experimental results of the snapshots $\hat{R}_i$ from six postures in one time window, using a $30 \times 18$ TagSheet. In this experiment, the threshold $R^T$ is set to $-100$ dBm and the length of time window is 3s. A snapshot is actually a gray-scale image that consists of $30 \times 18$ pixels. Each pixel $I_{m,n}$ in the image is the absolute value of the RSSI difference between $r^i_{m,n}$ and $r^0_{m,n}$, i.e., $I_{m,n} = |r^i_{m,n} - r^0_{m,n}|$. As we can see, each snapshot gives a blurring sketch of a sleeping posture. To figure out which posture each snapshot means, we need to overcome the following three challenges. First, due to the big physical size of tags, the image resolution of TagSheet is very low and most posture details are lost. Second, the RF signal is susceptible to surroundings. How to design a robust TagSheet that works properly under different environmental settings and for different users is a key problem. Third, apart from the traditional classifiers, how to characterize different postures with physical meanings and avoid tedious data training is also a challenging issue. Next, we discuss how to correlate snapshots to different postures.

### C. Image Processing

In identifying sleep postures, a key step of TagSheet is to pre-process each snapshot, including Gaussian blur, Ostu-based binary conversion of the gray-level image, and removal of scattered pixels. In image processing, a Gaussian blur is the result of blurring an image by a Gaussian function, which is widely used to reduce image noise. In TagSheet, a two-dimension Gaussian function $G(x, y)$ is adopted as follows:

$$G(x, y) = \frac{1}{2\pi\sigma^2} e^{-\frac{x^2+y^2}{2\sigma^2}}, \tag{2}$$

where $\sigma$ is the standard variance. Hence, we have the Gaussian matrix $B = \{b_{i,j}\} = G(i, j)$, where $-1 \le i, j \le 1$ and $\sigma = 0.5$. The blurring result is a new image $I' = \{I'(m, n)\}$:

$$I'(m, n) = \sum_{i=-1}^{1} \sum_{j=-1}^{1} I_{m+i,n+j} b_{1+i,1+j}. \tag{3}$$

As aforementioned, the RF signal is susceptible to surroundings and human body. It is easy to make the proposed recognition model over-fitting if the RSSI difference in each pixel is used directly. To address this problem and make TagSheet robust, we convert the gray-level image to a binary image with Otsu's method [12]. In computer vision, Otsu's method is used to automatically perform clustering-based image thresholding and reduce a gray-level image to a binary image. The algorithm assumes that the image contains two classes of pixels following bi-modal histogram (foreground pixels and background pixels). It then calculates the optimum threshold separating the two classes so that their intra-class variance is minimal and inter-class variance is maximal. Assume the foreground and background pixels are '1' and '0', respectively. Different body postures will have a great impact on both the number and the shape of '1' pixels. By observing the '1's in the binary image BW (black and white), it is promising to identify different sleeping postures.

As shown in Fig. 5 (b), we obtain a binary image BW (black and white) of the left foetus posture from Fig. 5(a), which is produced with blurring. Clearly, the foreground pixels and background pixels are well separated by Otsu's threshold, which helps remove noise and highlight the body posture. However, there are some scattered points (white pixels of '1's) that are caused by destructive interference of superposed signals. To get rid of this noise, we remove from the binary image BW all connected components of pixel '1's that have fewer than $P$ pixels, producing another binary image BW2. As shown in Fig. 5(c) where $P$ is 6, most scattered '1's are removed; only a clear body is left for following recognition.

### D. Hierarchical Recognition

TagSheet is designed to unobtrusively identify the six common sleeping postures (in Fig. 3) using the passive tag matrix. It can be viewed as a multinomial classification problem. In this subsection, we propose a multi-level hierarchical classification instead of doing a one-stop posture identification. There are two steps: conducting a coarse-grained posture partition first and then performing a fine-grained classification based on the previous partition results. First, we partition the six sleeping postures together with empty bed (denoted as *nobody*) into three general categories, i.e., $C_1$ ={*nobody*}, $C_2$ = {*supine, prone*}, and $C_3$ ={*left log, right log, left foetus, right foetus*}. The reason for this partition is that the numbers of pixel '1's vary a lot amongst the three general categories. For $C_1$, since nobody stays in bed, there is no pixel '1' in theory. For $C_2$, the postures of supine and prone have a greater contact area with the bed than $C_3$, which results in more pixel '1's. Hence, by doing this partition, we are able to distinguish $C_1$, $C_2$, and $C_3$ by counting the number of pixel '1's. Since people have different body size, TagSheet needs a snapshot of supine as reference, which is referred to as reference snapshot, denoted by $I^*$. The thresholds for $C_1$ and $C_3$ are set to $0.1\lambda(I^*)$ and $0.8\lambda(I^*)$, where $\lambda(\cdot)$ is the number of pixel '1's. Note that the reference snapshot $I^*$ is taken just once for each individual; this is the only initial input of our method, without any tedious training process required.

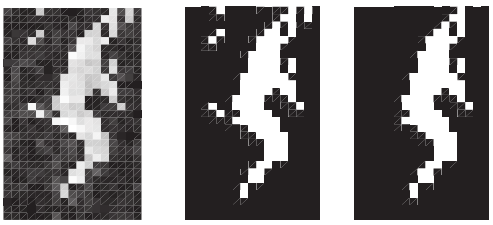

(a) Image $I'$ (b) Image BW (c) Image BW2

Fig. 5. Binary images of left foetus. (a) Gray-level image $I'$, (b) Otsu-based binary image BW, (c) image de-noising of BW.

For category $C_3$, we further divide the four sleeping postures into two subsets $C_{31}$ ={*left log, right log*} and $C_{32}$ = {*left foetus, right foetus*}. Compared to log posture, the body height of the foetus posture is smaller because the laid person curls his knees towards his chest. On the other hand, the image width of foetus is likely to be lager than that of log, which can be observed in Fig. 4, where the left log is 6 pixels in width and the left foetus is 8. However, there may be violations due to the interference from head, arms, and hands. For example, the image width of the right log in Fig. 4(d) is 10, which is more than that of the left foetus posture. To address this problem, we trim the image to half and just count the image width of the lower part of the body, which helps remove the arms and hands from the image and thereby avoids their negative interference. By using image width after trimming, we can easily distinguish between the foetus postures and the log postures based on the following metric:

$$\gamma = \frac{\psi_h}{\psi_w}, \tag{4}$$

where $\psi_h$ is the height of the body image and $\psi_w$ is the image width of the lower part of the body. The term $\gamma$ indicates the ratio of $\psi_h$ to $\psi_w$: the bigger the value of $\gamma$ is, the more likely the posture is a log. The threshold $T_\gamma$ is determined by the ratio of $\psi_h(I^*)$ to $\psi_w(I^*)$, where $I^*$ is the reference image. Since $I^*$ is the supine image, its height is close to that of log and larger than foetus; its width is larger than log and smaller than foetus. Thus, it is a natural threshold. Given an image in $C_3$, if $\gamma \geq T_\gamma$, it is a log. Otherwise, it is a foetus. The next is to recognize the individual posture in the three categories: $C_2$, $C_{31}$, and $C_{32}$, respectively.

*1) Supine vs. Prone:* In category $C_2$, supine and prone produce two very similar snapshots of the body shape due to the bilateral symmetry, which forms a great barrier to posture recognition. To overcome this challenge, we take a closer look at the pose difference between these two postures and find that the face in supine faces up while prone faces to left or right. This makes the head shape different and provides us with an opportunity to distinguish the two postures. From a top view, as shown in Fig. 6(a), the head width of the supine is less than prone, which leads to fewer pixel '1's when lying supine. In addition, the central axis of the head along Y-axis changes. The head axis and the body axis in supine coincide with each

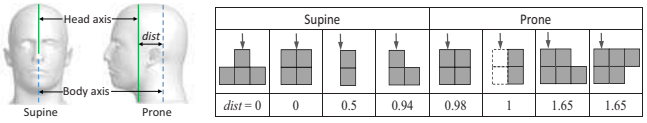


(a) (b)

Fig. 6. Supine vs. prone. (a) Top view of the head. (b) The common head pixels in supine and prone. The arrow ↓ is the body axis; the threshold of $dist$ to distinguish supine and prone is set to 0.95 when $\epsilon = 0.1$.

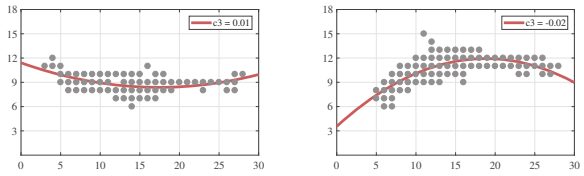


(a) Left log. (b) Right log.

Fig. 7. Quadratic regression of log postures.

other, namely, the distance $dist$ between the head axis and the body axis is zero. On the contrary, due to lying side, the head axis in prone deviates from the body axis, which forms a distance gap that can be used to identify prone.

Assume that the body lying in bed is parallel to the Y-axis (long axis of the bed).[1] The distance between the body axis and the head axis is actually the difference of X coordinates of these two lines. An intuitive way to obtain the body axis is to average the X coordinates of all pixel '1's. This works but not robust because the objective's limbs (arms and legs) may put anywhere and sometimes deviate the body axis from the ground truth. To address this issue, we run a linear filter again based on BW2 to remove the limbs from the body part. After that, only some scatters of limbs' pixels are left and we run Otsu's method [12] once again to obtain the binary image BW3 of the body shape. By averaging the X coordinates of pixel '1's in BW3, we are able to get an accurate estimate of the body axis that is close to the real value.

On the other hand, for the head axis, we expect to enlarge the impact of pixels far away from the body axis and suppress others (close to the body axis), which helps widen the gap of $dist$ between supine and prone. To do so, we weight each head pixel according to the distance between them and the body axis. The weight of the $i$-th head pixel is:

$$w_i = \frac{d_i^2 + \epsilon/k}{\sum_{i=1}^{k} d_i^2 + \epsilon}, \tag{5}$$

where $k$ is the number of head pixels, $d_i$ is the distance between the $i$-th head pixel and the body axis, $\epsilon$ is a small constant that ensures denominator is non-zero. With these weights, we are able to derive the head axis by computing $\sum_{i=1}^{k} w_i \times x_i$, where $x_i$ is the X coordinate of the $i$-th head pixel. Note that the head pixels are obtained by observing the first two rows of the body pixels. With the computed $dist$, a distance threshold is needed to distinguish between supine and prone. By observing more than 200 supine images and 200 prone images collected from 12 different volunteers, we find that the body axis and head pixels of supine and prone have a great difference. We divide these images into 8 general categories and a distance threshold 0.95 is found to determine the body postures, as shown in Fig. 6(b).

*2) Left Log vs. Right Log:* The log position in $C_{31}$ means that someone sleeps on his side with both legs straight. The most difference between the left log and the right log is that the person faces different orientation: the left and the right, respectively. If the feet are also taken into account, the log posture forms a 'bow'. By identifying the arc of the 'bow', we are able to distinguish between the left log and the right log. To do so, we first rotate the log image counterclockwise by 90°. After that, each pixel '1' is viewed as a point in the 2D plane and we perform the quadratic fitting on these scatters to obtain the orientation of the 'bow'. Assume the quadratic function is $y = \sum_{i=0}^{2} c_i x^i$, where $c_i$ is the coefficient, $x$ and $y$ are the coordinates of pixel '1's. The value of $c_2$ determines the orientation of the 'bow'. A positive $c_2$ means that the rotated 'bow' faces up, which further indicates that the raw 'bow' is towards left, namely, left log. Otherwise, the posture is the right log. Fig. 7 illustrates the quadratic regression of left log and right log after counterclockwise rotation by 90°.

*3) Left Foetus vs. Right Foetus:* Take a closer look at the foetus postures in $C_{32}$. The body profile of the left foetus in Fig. 4(e) looks like an 'S', while the right foetus is exactly a mirror image of 'S'. Similar to the log postures, we still adopt curve-fitting to distinguish the left foetus and the right foetus. To do so, we rotate the foetus image counterclockwise by 90° first. After that, we extract all pixel '1's from the image and perform the cubic polynomial fitting rather than the quadratic fitting on these pixels to obtain the function of the lying 'S'. Assume the cubic function is $y = \sum_{i=0}^{3} c_i x^i$, where $c_i$ is the coefficient, $x$ and $y$ are the coordinates of rotated image. The value of $c_3$ determines the shape of the lying 'S'. A negative $c_3$ presents a lying 'S' and indicates that the posture to be recognized is the left foetus. On the contrary, a positive $C_3$ plots a lying mirror image of 'S', which returns a result of the right foetus. Fig. 8 illustrates the cubic polynomial fitting.

### *E. Image Rotation*

During sleeping, the subject can be located anywhere on the bed at different lying angles. Hence, the raw snapshot is required to be standardized before posture recognition. Recalling the above hierarchical recognition, the body position on the bed has no effect on the recognition, but the rotation angle does. To avoid this side effect, we correct the rotated image and make the principal (major) axis of the body shape aligned vertically in the snapshot. The human body geometry is approximately treated as an ellipse and the angle $\alpha$ between the principal axis of the ellipse and the $Y$ axis is referred as to *rotation angle*. To derive $\alpha$, we find out the principal axis first by using principal components analysis (PCA). Given a binary image BW3, we get 2-dimension data that is made up of X-Y coordinates of pixel '1's. For PCA working properly, we subtract the mean from each of the data dimensions, where

[1] If not, we can rotate the body image by a proper angle, which will be discussed shortly later in Section II-E.

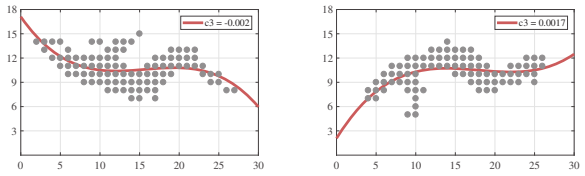


(a) Left foetus. (b) Right foetus.

Fig. 8. Polynomial curve fitting of foetus postures.

the mean is the average across each dimension. After that, we derive a covariance matrix:

$$C = \begin{pmatrix} cov(\mathbf{x},\mathbf{x}) & cov(\mathbf{x},\mathbf{y}) \\ cov(\mathbf{y},\mathbf{x}) & cov(\mathbf{y},\mathbf{y}) \end{pmatrix}, \quad (6)$$

where $\mathbf{x}$ is the set of $X$ coordinates, $\mathbf{y}$ is the set of $Y$ coordinates, and $cov(\mathbf{x},\mathbf{y})$ is the covariance of $\mathbf{x}$ and $\mathbf{y}$, i.e., $cov(\mathbf{x},\mathbf{y}) = \frac{\sum_{i=1}^{n}(x_i-\bar{\mathbf{x}})(y_i-\bar{\mathbf{y}})}{n-1}$. With $C$, we are able to calculate the eigenvectors and eigenvalues of this matrix. Between the two eigenvectors, the one with larger eigenvalue is the principal axis that characterizes the data.

### F. Posture Transition

So far, we have discussed the posture recognition of a still body. However, the person is likely to roll over when sleeping, which may make the sleeping posture 'blurred'. If we do not sweep out these posture transitions, multiple sleeping postures may coexist in a time window, which confuses the recognition and lowers the classification accuracy. As aforementioned, when a person lies in bed, the human body acts as "salt water" and is very likely to block the tags exactly beneath the body, which makes the reader fail to collect these tags. Hence, for each snapshot $R_i$, we just compare its blocked tags (pixels) with the previous one $R_{i-1}$, $i \geq 2$. If a posture transition happens, some previously unseen tags in $R_{i-1}$ will be queried by the reader in $R_i$ and also some unblocked tags turn out to be blocked. By counting the number of these changes, we are able to detect the posture transition easily. If the number is less than a threshold (e.g., 10% of the number of pixel '1's), we think the body is still. Otherwise, a posture transition happens and the snapshot is not taken into account.

### G. RF Radiation

One may concern whether it is safe to get exposed to RF radiation of an RFID reader when TagSheet is put into use. The answer is yes. Daniel W. Engels et al. [13] conduct extensive experiments and reveal that in an ideal absorption environment, an RFID reader located 10 centimeters (3.9 inches) from the human head presents a specific absorption rate of 2.0 W/kg, which is above the maximum value 1.6 W/kg allowed by the United States' Federal Communications Commission (FCC). To avoid any potential harm to humans, UHF RFID interrogators should be set back at least 0.5 meter (1.6 feet) from anyone who might receive constant exposure. For commercial interrogators, if they are kept at least 1 meter (3.3 feet) from the human body, the incident radiation – even on the eyes (the most vulnerable part of our bodies to RF radiation) – is at a level well below maximum allowable levels. In our TagSheet system, the reader (antenna) is deployed on ceiling, which is more than 2 meters (6.6 feet) apart from the human body. Hence, it is safe to use TagSheet.

## III. Respiration Rate

Besides sleeping postures, TagSheet can also estimate the respiration rate, not requiring any extra hardware setup.

### A. Basic Idea

A respiratory cycle consists of two processes: inhalation and exhalation. When inhaling, the diaphragm contracts and moves downward, which expands the lungs and enlarges the chest cavity. On the contrary, when exhaling, the diaphragm relaxes and moves upward, which contracts the lungs and reduces the space in the chest cavity. Hence, the breathing gives rise to the cyclic motion of chest, which further affects the tag's backscatter signal periodically. Based on this findings, we explore how to estimate the respiration rate with the phase shift. The reason why we take the phase rather than RSSI as the metric is that the phase has a fine-grained measure resolution and is more sensitive to the distance change. Estimating breathing rate, however, poses two challenges. First, due to the slight fluctuation of the chest, the phase shift caused by chest reflection is faint. We should carefully pick proper tags that can well present the phase variation and avoid the signal interference caused by occasional limb movement. Second, TagSheet consists of hundreds of tags and each is read in a round-robin way, which makes the sample rate low. Hence, how to estimate the breathing rate in the case of undersampling is another problem.

### B. Tag Selection

Intuitively, the signals of tags close to the chest are more susceptible to its cycle motion. Therefore, we are supposed to choose these tags as the vehicle to estimate the breathing rate. To do so, we first get the body image BW3 according to the approach mentioned in Section II-D1. After that, we pick out the tags that are located at the both sides of the body. For supine and prone, these tags are naturally candidates. For log and foetus, however, only one-side tags can be used. That is because, for example, when lying with left log, the chest motion takes place on the left of the body; the phase shifts of tags on the right side are negligible. By observing a selected tag for a period of time (e.g. one minute), we are able to get a phase profile of this tag, denoted by $\{(\theta_i, t_i)\}$, where $\theta_i$ is the $i$-th phase value measured by the reader at the time $t_i$.

Since the occasional limb movement during sleeping has a great impact on the phase measurement, a further check is needed to determine whether or not the selected tag can be added into the final list for breathing estimation. When the arm or leg moves, the phase will sharply jump and may remain stable at a new level later when the limbs are still again. To check these outliers, we resort to turkey's test [14].

Specifically, with the first quartile ($Q_1$) and the third quartile ($Q_3$) of all phases $\{\theta_i\}$, we get a turkey's range as follows:

$$[Q_1 - \rho(Q_3 - Q_1),\ Q_3 + \rho(Q_3 - Q_1)], \tag{7}$$

where $\rho = 3$ is a coefficient. If all phase values $\{\theta_i\}$ are bounded within this interval, no outliers happen and this tag is determined as the final candidate. Otherwise, it is wiped out. Note that, when collecting phase profile, we expect all things expect the chest are still. Hence, posture transition is not allowed within the assigned time window. Fortunately, the objective during sleeping keeps still in most cases; we can easily get a time window (e.g., 30s) without any posture transition. If a posture transition happens, we can easily detect it according to Section II-F and abandon the phase profile.

### C. Increasing Sample Rate

As mentioned above, due to the fixed read rate and a great number of tags in TagSheet, the phase profile is under sampling. A possible solution to this problem is compressive sensing (CS), which is a good vehicle to reconstruct a signal by solving underdetermined linear systems. Tagbeat [15] is the first work that uses CS to inspect high-frequency mechanical vibration and accurately estimate its period with relatively low RFID read rate. For our problem, however, since the respiration rhythm is not so steady as mechanical vibration, CS cannot fit well to the recovery of breathing signal. Hence, we resort to increasing the sample rate.

We observe that the under-sampling is due to the fact that the reader in TagSheet has to bear the strain of querying hundreds of tags concurrently. If only a small tag set is queried, the sample rate of each tag will see a sharp increase. Based on this observation, we pick only a few tags to reply and others are silenced. This can be implemented by carrying out the `Select` command. `Select` is a mandatory command in EPC Gen2 [16], which allows a reader to choose a specific subset of tags that participate in the subsequent query round. The selection principle is based on user-defined criteria, which follows Section III-B in this work. By this means, the sample rate will raise sharply. For example, the read throughput of Impinj R420 is more than 200 tags per second. If only 10 tags are selected, the average sample rate is 20 Hz, which is much greater than the twice of the breathing rate.

Note that, the improvement of sample rate is at the cost of silencing most tags. This will make the snapshot (shown in Fig. 4) fragmentary and disable TagSheet to identify sleeping postures. This is true if we individually check each snapshot. In practical use, however, we can address this problem by taking multiple snapshots into account. More specifically, once a sleep posture is identified, we switch to the mode of selective reading for more accurate breathing estimation. What about posture recognition? The answer is that we check the signals of selected tags in real time. If the body does not move, the signals vary slightly (caused by only noise and chest motion). In this case, we think the person keeps the same posture as before. Once a body move is detected, we quickly switch to the mode of normal reading, collect all tags, and execute the posture recognition as is.


Fig. 9. Experiment setup.

### D. Estimating Breathing Rate

With the oversampling breathing signals output by selective reading, we can run a discrete wavelet transform to remove the noises caused by imperfect hardware and surrounded environments, and pass the frequencies within a certain range. The frequency range is determined empirically according to the practical breathing rate. In statistics, the common breathing rate for an adult at rest ranges from 10 bpm to 20 bpm (breath per minute), and infants have higher breathing rate that is near 37 bpm. Hence, the respiration rate usually falls in the frequency range of [0.16, 0.62] Hz. With the wavelet filter, we are able to remove the residual noises by attenuating the signals with frequencies outside the frequency range of the breathing rate. After that, we conduct FFT on the filtered breathing signal and the peak of FFT outputs is the estimate of the breathing rate. Further more, we can run above approach on multiple selected tags and average the outcomes to get a more stable and accurate estimate of the breathing rate.

## IV. Evaluation

### A. Experiment Setup

As shown in Fig. 9, we deploy a $30 \times 18$ tag matrix on a thin plastic film, which is placed under the mattress and unobtrusive to users. The tag that we adopt is Impinj H47 [11] with the size of 5cm×5cm, and the interval between two adjacent tags is 2cm. Due to the low unit price of passive tags, this TagSheet cost only 30 dollars. Two Larid S9028 antennas mounted on the tripods (2.0 meters high) are uniformly scheduled by the Impinj Speedway R420 reader in a round-robin to ensure a full coverage of the tag matrix. We collected data from 12 different individuals, whose height ranges from 155 cm to 185 cm, and weight from 42 kg to 87 kg, as shown in Fig. 10. Each individual simulates his sleeping habits by lying on bed for a period of time and performing the six postures that he is used to when he goes to bed. All the input of TagSheet for each individual is only a 3-second reference snapshot $I^*$, without any data training. The ground truth is recorded by a camera and checked manually.

### B. Posture Recognition

*1) Image Rotation:* We now verify the PCA-based rotation algorithm, which is the precondition required by TagSheet.

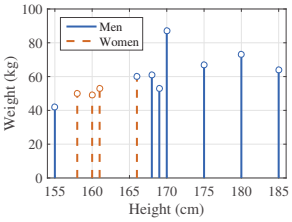


Fig. 10. Height and weight.

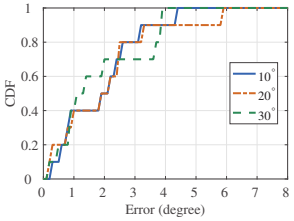


Fig. 11. Image-rotation accuracy.

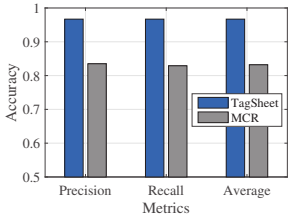


Fig. 12. TagSheet vs. MCR.

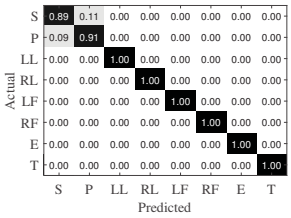


Fig. 13. Confusion matrix.

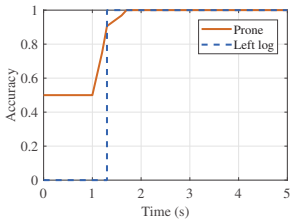


Fig. 14. Impact of window size.

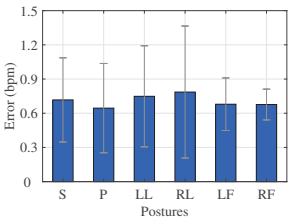


Fig. 15. Breathing estimate.

In the experiment, the supine posture is adopted by the volunteers. The reason why not choose the other postures is that prone has a very similar snapshot as supine due to the bilateral symmetry, and the ground truth of the body axes of the other four postures is hard to measure, especially for foetus. In each experiment, the volunteers carefully adjust their body axes to make them rotate at three particular angles 10°, 20°, and 30°. For a fixed angle, 12 volunteers repeat the experiment ten times and there are 120 outputs in total. Fig. 11 plots the CDF of angle errors of the PCA-based algorithm. The experimental results show that the means of the degree errors in the three cases are about 2.0° and the 90th percentiles are less than 5.7°. This good performance indicates that the PCA-based image-rotation approach is able to achieve accurate angle estimate, which paves the way on robust posture recognition for any rotated body shapes.

*2) Identification Accuracy:* Fig. 12 compares the precision and recall results of six posture identification with the recent work minimum class residual (MCR) [4] that uses pressure mapping to recognize the same six postures as our work. In this figure, the average is the arithmetic mean of precision and recall. We note that the precision of TagSheet for classifying six postures reaches up to 96.7%, which is far superior to MCR (83.5%). The similar conclusion can also be drawn for recall, which well indicates the great performance of our hierarchical recognition scheme. In Fig. 13, we show the confusion matrix of six postures supine (S), prone (P), left log (LL), right log (RL), left foetus (LF), right foetus (RF), together with empty bed (E) and posture transition (T). As we can see, the side postures left log, right log, left foetus, right foetus, are all classified correctly with certainty, which demonstrates that the geometric features characterized by our approach can well reflect these postures and the polynomial curve fitting is effective. On the contrary, the supine and prone have about 10% chance to be erroneously classified into the other. That is because these two postures have extremely similar snapshots due to the bilateral symmetry.

*3) Length of Time Window:* In Fig. 14, we study the impact of time window size on the accuracy of posture recognition. For the sake of clarity, we pick two sleeping postures, prone (similar to supine) and left log (similar to other side lying postures) as the representative. We can see that the identification accuracy remains stable at first. That is because, with the TagSheet having 540 tags, the short window will make the reader collect only a small number of tags, which cannot form a clear RF snapshot. The reason for prone's high starting point is that we distinguish between prone and log by counting the number of pixel '1's. If a tag has not been read yet, it is treated as a pixel '1', which leads to that all postures are mistakenly treated as supine and prone. After that, with the increase of time window, more tags are read and a clear RF snapshot appears, leading to a sharp rise of the accuracy. Once the whole snapshot is taken, more readings do not contribute any additional information to the posture identification, and the accuracy remains stable henceforth. Hence, in our experiments, we set window size to 3s for the best performance and the minimal delay. We believe that this delay is sufficient to support many medical applications and avoid the risk caused by improper postures.

### C. Breathing Rate

Breathing rate is a useful diagnostic indicator that can assess the personal physical health and provide prompts to chronic diseases. We now study the estimation accuracy of breathing rate by incorporating the method of selective reading and the technology of wavelet transform. Fig. 15 compares the mean errors of the estimation under six sleeping postures. As we can see, the mean error is around 0.7 bpm (breath per minute), which well indicates that, as a by-product, Tag-Sheet can estimate the respiration rate accurately. It is interesting that prone has a higher accuracy than others. One possible reason is that, a respiratory cycle consists of inhalation and exhalation, which gives rise to the cyclic chest motion and further affects the tag's backscatter signal. When lying prone, the chest cavity is oppressed, which makes the breathing more heavily than others for getting enough oxygen and thereby produces more signal interferences, increasing the signal-to-noise ratio and benefiting the signal recovery.

## V. Related Work

Sleep is a major part of health and well-being. Existing sleep monitoring works fall into two broad categories: sleep quality analysis [17], [18], [19], [20], [21], [22] and sleeping posture recognition [6], [23], [7], [4], [8]. The former is to analyze the sleep status, aid in the medical diagnosis

of diverse sleep and psychiatric disorders, and serve as an indicator of chronic diseases. iSleep [17] uses acoustic signals of a smart phone to detect various sleep-related events, such as body movement, couch, and snore. MASC [19] achieves accurate and robust stage classification by using the brain and myoelectric signals taken from a mouse. Recent works try to use breathing rate information to get a fine-grained sleeping analysis [20], [21]. SleepSense [22] adopts a doppler radar-based sensor to recognize not only the breathing rate, bus also on-bed movement. MotionScale [24] is a motion detection system based on low-cost load cell sensors. By observing the electrical resistance changes on each load cell, MotionScale is able to infer possible body motions on the bed. Although these approaches are proposed to monitor sleep quality accurately, they cannot figure out the still sleeping postures.

Sleeping posture recognition is to identify the body postures on bed during sleep, which is helpful for assessing personal physical health and giving prompts to chronic diseases. Early research [6], [23] focuses on the posture recognition by observing cardiovascular signals, such as electrocardiogram. To get these data, the specialized medical instrument is needed, which requires professional operations and thus is expensive to use. Video cameras, as another vehicle, have also been used previously to recognize the sleeping postures [7]. These image-based approaches work but suffer from privacy concerns and low-light noise. Besides, the posture images cannot be captured if the body is covered by quilt. Recent research has shifted to the pressure sensing techniques [4], [8]. By designing a dense pressure sensitive bedsheet with dispersed textile sensors, they are able to capture the pressure mapping images and recognize different postures by using classifiers. However, the deployment of pressure sensor mat affects the sleeping comfort and is not a non-intrusive solution. Besides, the pressure sensor cannot be self-energized; a power supply or batteries are needed, which increases the deployment cost and the maintenance overhead.

## VI. Conclusion

This paper presents a sleep monitoring system called TagSheet that can not only identify the body posture on bed, but also estimate the respiration rate. By extracting geometric features from the RF snapshots and using the hierarchical recognition scheme, TagSheet is able to accurately identify the sleeping postures in a plug-and-play way, without any tedious data training. Besides, a tag selection approach and wavelet-filter based technology are presented to estimate the respiration rate. Experiment results show that TagSheet has a great performance.

## Acknowledgment

This work is supported by Natural Science Foundation of Jiangsu Province (BK20170648), National Natural Science Foundation of China (61702257, 61771236, 61772251), Jiangsu Key R&D Plan (Industry Foresight and Common Key Technology, BE2017154), Project funded by China Postdoctoral Science Foundation, US National Science Foundation CNS-1718708, Fundamental Research Funds for the Central Universities, and Collaborative Innovation Center of Novel Software Technology and Industrialization. Jia Liu and Lijun Chen are corresponding authors.

## References

[1] U. D. of Health, H. Services *et al.*, "How many infants die from SIDS or are at risk for SIDS?" 2014.
[2] R. M, G. SS, and R. PA, "Preventing pressure ulcers: A systematic review," *JAMA*, vol. 296, no. 8, pp. 974–984, 2006.
[3] U. D. of Health, H. Services *et al.*, "Sleep apnea: what is sleep apnea?. health information for the public nhlbi," 2010.
[4] J. J. Liu, W. Xu, M.-C. Huang, N. Alshurafa, M. Sarrafzadeh, N. Raut, and B. Yadegar, "Sleep posture analysis using a dense pressure sensitive bedsheet," *Pervasive and Mobile Computing*, vol. 10, pp. 34 – 50, 2014.
[5] A. Menon and M. Kumar, "Influence of body position on severity of obstructive sleep apnea: A systematic review," *ISRN Otolaryngology*, 2013.
[6] H. J. Lee, S. H. Hwang, S. M. Lee, Y. G. Lim, and K. S. Park, "Estimation of body postures on bed using unconstrained ecg measurements," *IEEE journal of biomedical and health informatics*, vol. 17, no. 6, pp. 985–993, 2013.
[7] T. Grimm, M. Martinez, A. Benz, and R. Stiefelhagen, "Sleep position classification from a depth camera using bed aligned maps," in *Proc. of IEEE ICPR*, 2016, pp. 319–324.
[8] S. Ostadabbas, M. B. Pouyan, M. Nourani, and N. Kehtarnavaz, "In-bed posture classification and limb identification," in *Proc. of IEEE BioCAS*, 2014, pp. 133–136.
[9] Y. Hou, Y. Wang, and Y. Zheng, "Tagbreathe: Monitor breathing with commodity RFID systems," in *Proc. of IEEE ICDCS*, 2017, pp. 404–413.
[10] C. Idzikowski, *Beating Insomnia: How to Get a Good Night's Sleep*. Gill & Macmillan Ltd, 2003.
[11] Impinj Inc., *http://www.impinj.com*, 2018.
[12] N. Otsu, "A threshold selection method from gray-level histograms," *IEEE Transactions on Systems, Man, and Cybernetics*, vol. 9, no. 1, pp. 62–66, 1979.
[13] D. D. Arumugam and a. D. W. Engels, "Impacts of RF radiation on the human body in a passive RFID environment," in *IEEE Antennas and Propagation Society International Symposium*, 2008, pp. 1–4.
[14] W. Haynes, *Tukey's Test*. Springer New York, 2013, pp. 2303–2304.
[15] L. Yang, Y. Li, Q. Lin, X.-Y. Li, and Y. Liu, "Making sense of mechanical vibration period with sub-millisecond accuracy using backscatter signals," in *Proc. of ACM Mobicom*, 2016, pp. 16–28.
[16] "EPC radio-frequency identity protocols generation-2 UHF RFID standard," GS1, ISO/IEC 18000-63, 2018.
[17] T. Hao, G. Xing, and G. Zhou, "iSleep: unobtrusive sleep quality monitoring using smartphones," in *Proc. of ACM Sensys*, 2013, pp. 4:1–4:14.
[18] L. Samy, M. C. Huang, J. J. Liu, W. Xu, and M. Sarrafzadeh, "Unobtrusive sleep stage identification using a pressure-sensitive bed sheet," *IEEE Sensors Journal*, vol. 14, no. 7, pp. 2092–2101, 2014.
[19] Y. Suzuki, M. Sato, H. Shiokawa, M. Yanagisawa, and H. Kitagawa, "MASC: Automatic sleep stage classification based on brain and myoelectric signals," in *Proc. of IEEE ICDE*, 2017, pp. 1489–1496.
[20] Y. Ren, C. Wang, J. Yang, and Y. Chen, "Fine-grained sleep monitoring: Hearing your breathing with smartphones," in *Proc. of IEEE INFOCOM*, 2015, pp. 1194–1202.
[21] J. Liu, Y. Wang, Y. Chen, J. Yang, X. Chen, and J. Cheng, "Tracking vital signs during sleep leveraging off-the-shelf wifi," in *Proc. of ACM Mobihoc*, 2015, pp. 267–276.
[22] F. Lin, Y. Zhuang, C. Song, A. Wang, Y. Li, C. Gu, C. Li, and W. Xu, "SleepSense: A noncontact and cost-effective sleep monitoring system," *IEEE transactions on biomedical circuits and systems (TBIOCAS)*, vol. 11, no. 1, pp. 189–202, 2017.
[23] A. Supratak, H. Dong, C. Wu, and Y. Guo, "DeepSleepNet: a model for automatic sleep stage scoring based on raw single-channel eeg," *IEEE Transactions on Neural Systems and Rehabilitation Engineering (TNSRE)*, 2017.
[24] M. Alaziz, Z. Jia, J. Liu, R. Howard, Y. Chen, and Y. Zhang, "Motion scale: A body motion monitoring system using bed-mounted wireless load cells," in *Proc. of IEEE CHASE*, 2016, pp. 183–192.